DOI: 10.3901/CJME.2015.0317.032, available online at www.springerlink.com; www.cjmenet.com; www.cjme.com.cn

Control Algorithm of Electric Vehicle in Coasting Mode Based on Driving Feeling

SUN Daxu[1, 2], LAN Fengchong[1, 2], ZHOU Yunjiao[1, 2, *], and CHEN Jiqing[1, 2]

1 *School of Mechanical & Automotive Engineering, South China University of Technology, Guangzhou 510640, China*
2 *Key Laboratory of Guangdong Province of Automotive Engineering, South China University of Technology, Guangzhou 510640, China*

Received July 24, 2014; revised March 10, 2015; accepted March 17, 2015

Abstract: Coasting in gear is a common driving mode for the conventional vehicle equipped with the internal combustion engine (ICE), and the assistant braking function of ICE is utilized to decelerate the vehicle in this mode. However, the electric vehicle (EV) does not have this feature in the coasting mode due to the relatively small inertia of the driving motor, so it will cause the driver cannot obtain the similar driving feeling to that of the conventional vehicle, and even a traffic accident may occur if the driver cannot immediately adapt to the changes. In this paper, the coasting control for EV is researched based on the driving feeling. A conventional vehicle equipped with continuously variable transmission (CVT) is taken as the reference vehicle, and the combined simulation model of EV is established based on AVL CRUISE and MATLAB/Simulink. The torque characteristic of the CVT output shaft is measured in coasting mode, and the data are smoothed and fitted to a polynomial curve. For the EV in coasting mode, if the state of charge (SOC) of the battery is below 95%, the polynomial curve is used as the control target for the torque characteristic of the driving motor, otherwise, the required torque is replaced by hydraulic braking torque to keep the same deceleration. The co-simulation of Matlab/Simulink/Stateflow and AVL CRUISE, as well as the hardware-in-loop experiment combined with dSPACE are carried out to verify the effectiveness and the real-time performance of the control algorithm. The results show that the EV with coasting braking control system has similar driving feeling to that of the reference vehicle, meanwhile, the battery SOC can be increased by 0.036% and 0.021% in the initial speed of 100 km/h and 50 km/h, respectively. The proposed control algorithm for EV is beneficial to improve the driving feeling in coasting mode, and it also makes the EV has the assistant braking function.

Keywords: electric vehicle, coasting braking, control algorithm, engine braking, motor braking

1 Introduction

Electric vehicles (EVs) are suitable for urban conditions because of its lower speed, shorter driving range and non-pollution compared to conventional internal combustion engine (ICE) vehicles[1–2]. In urban traffic, the working conditions change frequently among acceleration, deceleration, parking and starting[3]. For the conventional vehicle with ICE, the decelerating situation includes coasting in gear and braking. In the coasting mode, the assistant braking function of the ICE[4] is utilized to decelerate the vehicle, and the driving feeling associated with the speed and the deceleration change during the process is important for the driver to avoid traffic accidents. However, EVs do not have the function due to the small inertia of the driving motor, so the driver who is used to the conventional vehicle may not be able to adapt to the EV immediately, and even traffic accidents may occur, such as rear collision, running through the red lights and braking emergently, etc. So, it's very important for EVs to retain the similar driving feeling to that of conventional vehicles in coasting mode. Moreover, recovery of braking energy is the main energy-saving method for an EV[5–6]. For EVs, the assistant braking which can be achieved by motor braking not only can improve the driving feeling in coasting mode, but also recover part of the braking energy.

Some scholars have conducted massive research works in the domain of regenerative braking and control of EVs. XU, et al[7], proposed a fuzzy-logic based regenerative brake strategy, and achieved high quality performance. BO, et al[8], proposed H^{∞} robust control strategy for regenerative brake torque control, which improved control unit's ability to resist disturbance. YANG, et al[9], proposed a control strategy to maximize the recovery braking energy, and the sequential quadratic programming technique is applied to optimize the braking torque. Most studies mentioned above mainly focus on regenerative brake when the vehicles are in deceleration condition, while the regenerative brake in coasting mode is seldom researched.

* Corresponding author. E-mail: mezhouyj@scut.edu.cn
Supported by Guangdong Provincial Science and Technology Planning Project of China (Grant Nos. 2013B010402006, 2013B010405007, 2013B090600024)

It has been proved that the coasting mode of the vehicle accounts for about 14% of the entire urban cycle[10]. WANG, et al[11−12], researched the regenerative braking of hybrid electric vehicle (HEV) in coasting mode. An electric motor torque optimization control algorithm was proposed to maximize the recovered power, and the corresponding optimal shift-control rule of the automatic transmission was obtained. SUN, et al[13], introduced a control algorithm according to the target brake distance in coasting mode for a HEV with the gear box at the neutral position, which is not common in real conditions. Based on various vehicle attributes, CIKANEK, et al[14], discussed a new improved parallel regenerative braking system for a PHEV to maximize the regenerative braking force without adding additional cost. For pure electric vehicles, only a few researchers studied the regenerative braking in coasting mode. LU, et al[15], studied the regenerative braking during coasting process, but the driving feeling is not taken into consideration. CHEN, et al[16], proposed the adaptive-learning regeneration control for the EV in coasting mode, but the control algorithm needs large amount of calculation and is not suitable for real time control.

In the literatures mentioned above, the research works are mainly focused on regenerative brake, but the driving feeling is seldom considered during coasting process, especially for EVs. In this research, the coasting control algorithm is proposed to obtain the similar driving feeling to that of the ICE vehicle. The main works include the coasting characteristic simulation of the reference vehicle, the establishment of the EV simulation model, the control strategy development in coasting mode, the analysis and discussion of the simulation and hardware-in-loop experiment results.

2 Drive System Layout and Parameters of the Reference Vehicle

A small-sized front-wheel drive ICE vehicle, whose transmission system is mainly composed of an engine, a torque converter, a CVT, a main reducer, a differential is taken as the reference vehicle. The transmission system of the vehicle is shown as Fig. 1. The vehicle parameters are listed in Table 1. The input and output characteristics of the torque converter are shown in Fig. 2 and the CVT transmission ratios and shift schedule are shown as Fig. 3.

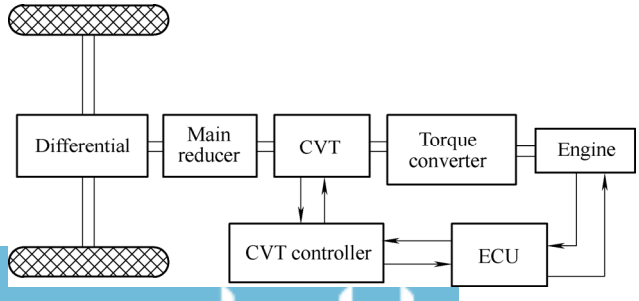

Fig. 1. Drive system layout of the reference vehicle

Table 1. Main parameters of the reference vehicle

Parameter	Value
Curb weight m/kg	910.00
Drag coefficient c	0.33
Frontal area A/m^2	1.72
Wheel dynamic rolling radius R/m	0.264
Final drive transmission ratio i	3.40
Engine displacement V/cm^3	1186.00
Engine working temperature t/℃	80.00

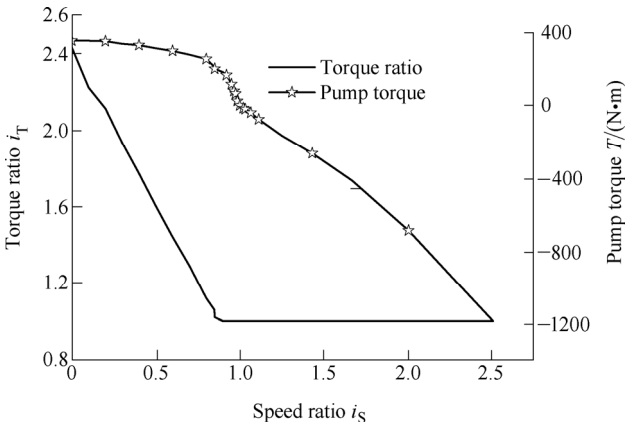

Fig. 2. Input and output characteristics of the torque converter

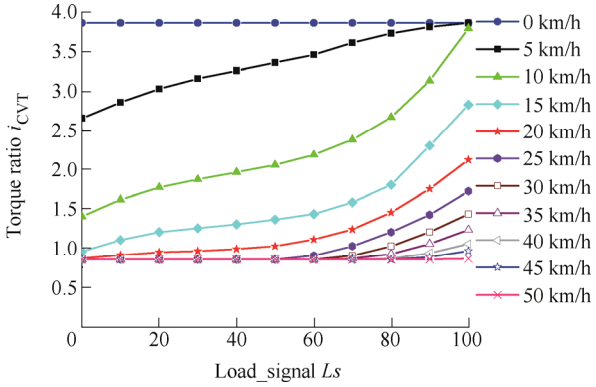

Fig. 3. CVT transmission ratios and shift schedule

3 Torque Characteristics of CVT Output Shaft for the Reference Vehicle

Due to the similar specifications and characteristics of main reducer, differential and the wheels used in the EV with the reference vehicle, just the torque characteristic at the output shaft of the CVT need to be studied:

$$T_{CVT} = T_{ENG} i_{CON} i_{CVT} \eta_T, \tag{1}$$

where T_{CVT} is the output torque of the CVT, T_{ENG} is the engine torque, i_{CON} and i_{CVT} is the transmission ratio of the torque converter and the CVT respectively, η_T is the total transmission efficiency.

Assuming the operating temperature of the engine is constant and the engine throttle opening is zero when the vehicle is in coasting condition, then Eq. (1) can be rewritten as Eq. (2):

$$T_{CVT} = f(n_{CVT}), \tag{2}$$

where n_{CVT} is the output rotation speed of the CVT.

The simulation model of the reference vehicle is established in the AVL CRUISE environment and the coasting task is set. In the coasting task, firstly the vehicle is accelerated with full load for two seconds at a certain initial speed, secondly the accelerator pedal is released gradually till the engine throttle opening is zero, and then the vehicle begins the coasting mode. The variable *Ls* is defined to represent the load signal associated with the accelerator pedal position. Fig. 4 shows the operating mode designed in MATLAB/Simulink.

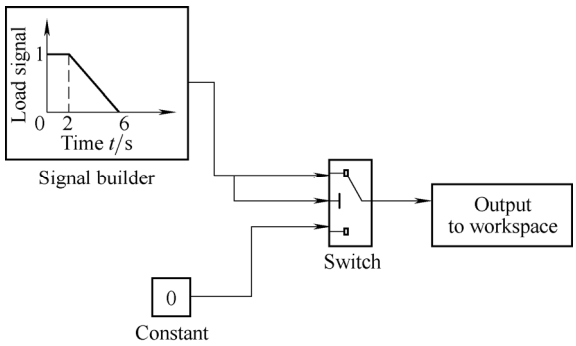

Fig. 4. Operation mode designed in MATLAB/Simulink

Because the speed of a vehicle is generally less than 100 km/h in urban cycle, so the maximum initial speed of the reference vehicle is set to 100 km/h. The braking energy cannot be recycled by driving motor of the EV when the vehicle speed is less than 10 km/h, thus the minimum speed is set to10 km/h.

Fig. 5 shows the torque characteristic of the CVT output shaft with rotation speed when the vehicle is in coasting mode (*Ls*=0). The original data are collected from the experiment, then smoothed and polynomially fitted using MATLAB software. The obtained polynomial is shown as Eq. (3):

$$\begin{aligned} f(n_{CVT}) = &-1.889\times10^{-22}\times n_{CVT}^7 + \\ &3.449\times10^{-18}\times n_{CVT}^6 - 2.628\times10^{-14}\times n_{CVT}^5 + \\ &1.075\times10^{-10}\times n_{CVT}^4 - 2.519\times10^{-7}\times n_{CVT}^3 + \\ &3.293\times10^{-4}\times n_{CVT}^2 - 0.209\,6\times n_{CVT} - 33.81. \end{aligned} \tag{3}$$

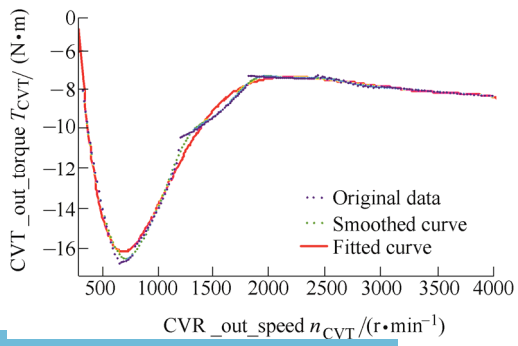

Fig. 5. Torque characteristic of CVT output of reference vehicle

4 Layout and Main Parameters of the Developed EV

The transmission system of the developed EV is shown as Fig. 6. It is mainly composed of a driving motor, a main reducer, a differential, four wheels, a motor controller, a brake controller and the battery pack. The main parameters of the EV are listed in Table 2.

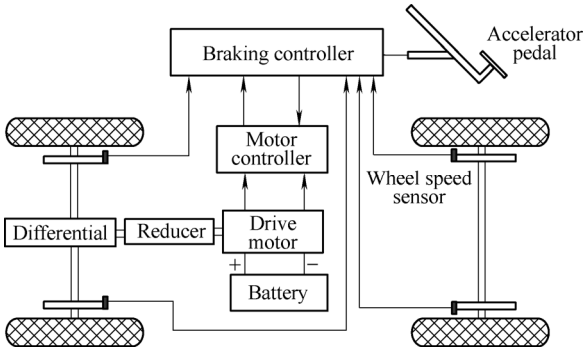

Fig. 6. Layout of the developed EV

Table 2. Whole-vehicle parameters of the developed EV

Parameter	Value
Curb weight m/kg	1310
Drag coefficient c_d	0.33
Frontal area A/m^2	1.72
Wheel dynamic rolling radius R/m	0.264
Final drive transmission ratio i_F	3.4
Centroid height h_g/m	0.56
Distance from centroid to front axle a/m	1.087
Distance from centroid to rear axle b/m	1.603
Wheelbase L/m	2.690
Motor's rated voltage U_e/V	288
Motor's rated power P_e/kW	15
Motor's maximum power P_m/kW	30

5 Coasting Brake Control Algorithm for the Developed EV

5.1 Torque characteristic of the driving motor in coasting mode

When the vehicle is in coasting mode, the relationship between the rotation speed of the driving motor $n_{mot}(t)$ and the speed of the EV $V(t)$ is expressed by Eq. (4):

$$n_{mot}(t) = \frac{V(t)}{R}\times i, \tag{4}$$

where R is the dynamic rolling radius of the driving wheels, i is the transmission ratio of the EV transmission system.

In order to achieve the similar driving feeling to that of the reference vehicle, the demanded torque of the driving motor $T_{req}(t)$ can be expressed by Eq. (5) according to Eq. (3):

$$T_{\mathrm{req}}(t)=f(n_{\mathrm{mot}}(t))=-1.889\times10^{-22}\times(n_{\mathrm{mot}}(t))^7+3.449\times10^{-18}\times(n_{\mathrm{mot}}(t))^6-2.628\times10^{-14}\times(n_{\mathrm{mot}}(t))^5+1.075\times10^{-10}\times(n_{\mathrm{mot}}(t))^4-2.519\times10^{-7}\times(n_{\mathrm{mot}}(t))^3+3.293\times10^{-4}\times(n_{\mathrm{mot}}(t))^2-0.2096\times n_{\mathrm{mot}}(t)-33.81. \quad (5)$$

The load signal Ls of the driving motor is gained by Eq. (6):

$$Ls(t)=\frac{T_{\mathrm{req}}(t)}{T_{\mathrm{motmax}}(n_{\mathrm{mot}}(t))}\times100\%, \quad (6)$$

where T_{motmax} is the maximum torque of the driving motor.

If the demanded torque is greater than the maximum torque that the driving motor can provide, then the braking torque is supplied by the hydraulic braking system.

For a disk brake, the braking torque M_{B} generated under a certain pressure p_{B} can be expressed by Eq. (7):

$$M_{\mathrm{B}}=2p_{\mathrm{B}}\times A_{\mathrm{B}}\times\eta_{\mathrm{B}}\times\mu_{\mathrm{B}}\times r_{\mathrm{B}}\times C_{\mathrm{B}}, \quad (7)$$

where p_{B}—Pressure of the hydraulic,
A_{B}—Brake piston surface,
η_{B}—Efficiency,
μ_{B}—Friction coefficient,
r_{B}—Effective friction radius,
c_{B}—Specific brake factor.

The left and the right hydraulic brake system of each vehicle axle have identical size and attribute. Thus the demanded pressure $p_{\mathrm{req}}(t)$ can be calculated by Eq. (8). In Eq. (8), the subscript f and r represent the front and rear axle respectively:

$$p_{\mathrm{req}}(t)=\frac{T'_{\mathrm{req}}(t)}{4(A_{\mathrm{Bf}}\times\eta_{\mathrm{Bf}}\times\mu_{\mathrm{Bf}}\times r_{\mathrm{Bf}}\times C_{\mathrm{Bf}}+A_{\mathrm{Br}}\times\eta_{\mathrm{Br}}\times\mu_{\mathrm{Br}}\times r_{\mathrm{Br}}\times C_{\mathrm{Br}})}, \quad (8)$$

where

$$T'_{\mathrm{req}}(t)=\begin{cases}0, & \text{when regenerative braking enable,}\\ T_{\mathrm{req}}(t), & \text{when regenerative braking disable.}\end{cases}$$

5.2 Development of the coasting braking control algorithm for the EV

The effect of battery SOC on feedback braking is taken into account to avoid overcharge, and the regenerative braking is disabled when the SOC is above 95%. In order to avoid frequent switch between enabling and disabling of the regenerative braking, the regenerative braking is kept disabled until the SOC is less than 90%. The demanded braking torque is provided by the hydraulic braking when the regenerative braking function is disabled. The control algorithm developed in Matlab/Simulink/Stateflow for coasting braking of the EV is shown as Fig. 7. The input parameters of the control system are the driving motor speed, the maximum brake torque of the driving motor at current time, the speed of the EV, the pressure signal of the hydraulic system and the SOC of the battery pack. The output parameters of the system are the demanded pressure in the hydraulic system, the demanded load signal and torque of the driving motor. The coasting control system is activated when the accelerator pedal is completely released. Fig. 8 shows the coasting control subsystem in detail.

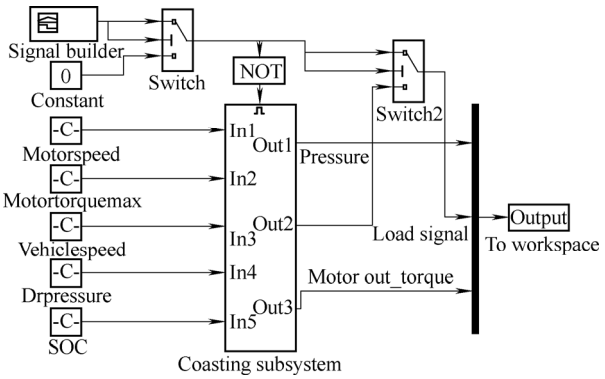

Fig. 7. Coasting control algorithm for the EV

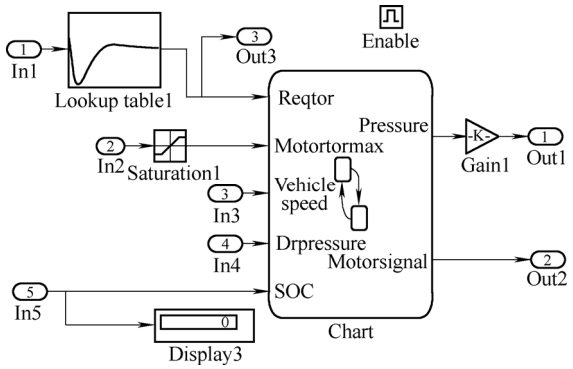

Fig. 8. Coasting control subsystem

6 Simulation Result Analysis

The simulation of the EV is performed with the same coasting task of the reference vehicle defined above. The co-simulation of AVL CRUISE and Matlab/Simulink is carried out to research the consistency of the velocity and acceleration between the EV and the reference vehicle on condition of different initial speed as well as battery SOC. The simulation step is set to 0.001 s.

6.1 Result analysis of the motor braking with SOC 60%

The comparisons between the EV without braking control and the reference vehicle in coasting mode in the initial speed of 100 km/h and 50 km/h are shown as Fig. 9, Fig. 10, respectively.

From Fig. 9(a) and Fig. 10(a), it is evident that the difference of the speed is increasing with the coasting time, and the speed of the reference vehicle decreases more quickly due to the additional engine braking besides the common driving resistance, i.e., the air resistance, the tire rolling resistance, etc. Correspondingly, the deceleration of

the reference vehicle is larger than that of the EV, as shown in Fig. 9(b) and Fig. 10(b). Due to the great differences of the speed and acceleration between the reference vehicle and the EV, the driving feeling of the two vehicles is remarkably different.

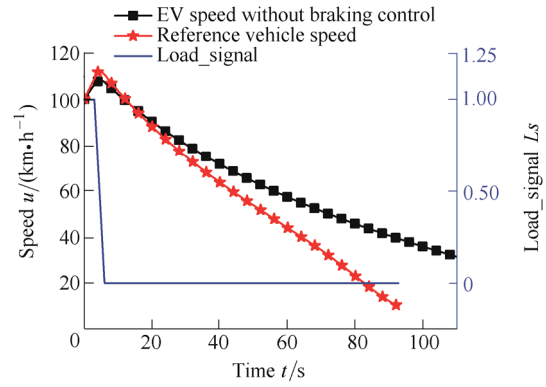

(a) Speed contrast

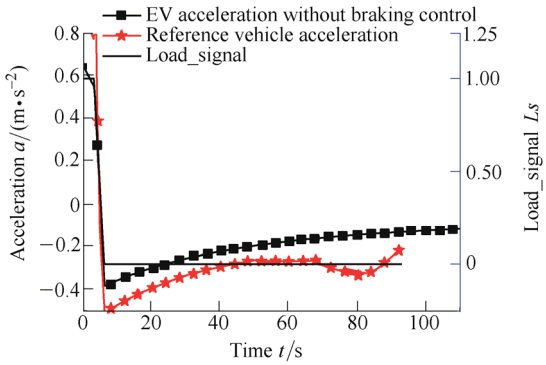

(b) Acceleration contrast

Fig. 9. Simulation results of reference vehicle and EV without braking control at initial speed of 100 km/h

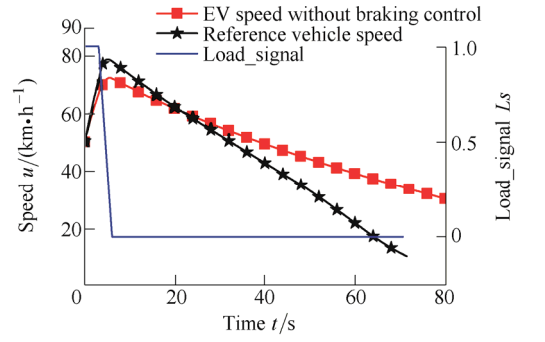

(a) Speed contrast

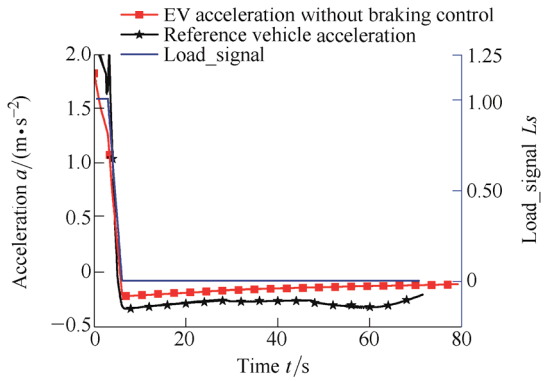

(b) Acceleration contrast

Fig. 10. Simulation results of reference vehicle and EV without braking control at initial speed of 50 km/h

Fig. 11 and Fig. 12 show the simulation results comparison at the initial speed of 100 km/h and 50 km/h, respectively for the reference vehicle and the EV with coasting braking control.

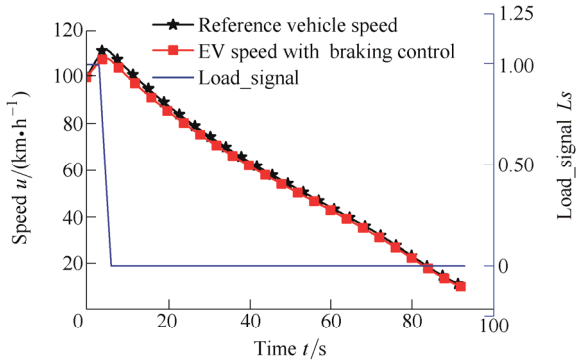

(a) Speed contrast

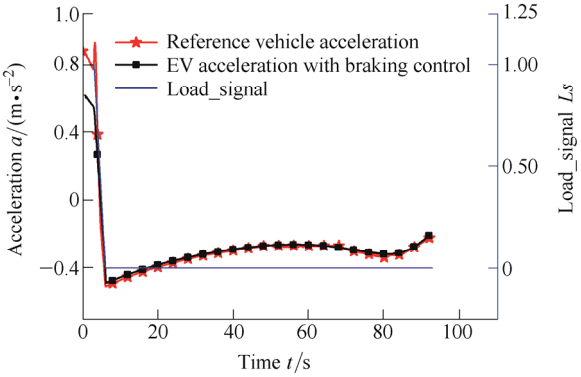

(b) Acceleration contrast

Fig. 11. Simulation results of reference vehicle and EV with braking control at initial speed of 100 km/h

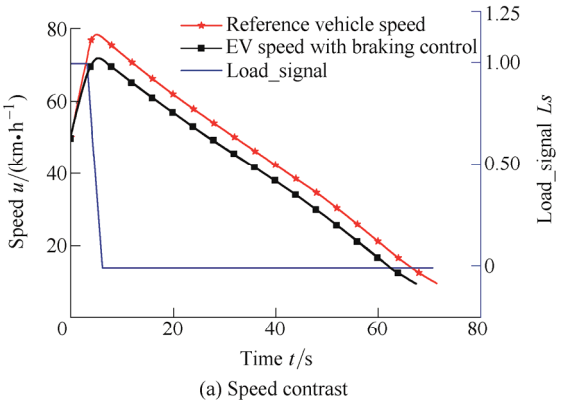

(a) Speed contrast

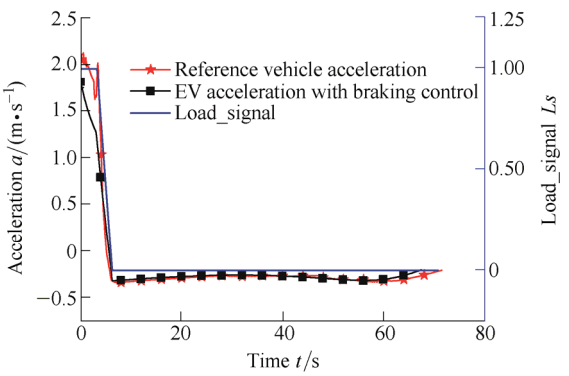

(b) Acceleration contrast

Fig. 12. Simulation results of reference vehicle and EV with braking control at initial speed of 50 km/h

Fig. 11(a) shows that the speed of the reference vehicle is slightly higher than that of the EV after the full-load acceleration (Ls=1) due to the better acceleration performance of the reference vehicle. After the accelerator pedal is entirely released (Ls=0), the two speed curves are almost parallel. The two acceleration curves are almost coincident after the accelerator pedals are completely released, as shown in Fig. 11(b). It means that the similar coasting driving feeling can be achieved for the EV compared to the reference vehicle.

Fig. 13 shows the battery SOC changes of the EV with coasting braking control at the initial speed of 100 km/h and 50 km/h, respectively. At the beginning of simulation, the SOC has a rapid decline because of the full load acceleration. When the accelerator pedal is released entirely (Ls=0) and the regenerative braking is active, the SOC begins slowly rising. The changes of the SOC are shown in Table 3 in the process of the regenerative braking. It can be seen that the SOC increased by 0.036% and 0.021 2%, respectively at the two initial speeds, so the effectiveness of the regenerative braking is confirmed.

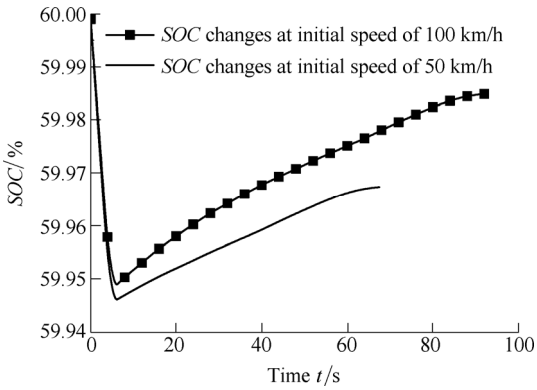

Fig. 13.　SOC changes of the battery

Table 3.　SOC changes during coasting process

Initial speed u/(km • h^{-1})	Start_coasting SOC SOC/%	Final SOC SOC/%	SOC change ΔSOC/%
100	59.948 9	59.984 9	0.036 0
50	59.946 1	59.967 3	0.021 2

6.2　Results analysis of the hydraulic coasting braking with SOC 96%

When the SOC is above 95%, the battery cannot be charged and the function of regenerative braking of the EV is disabled. So the demanded braking torque of the EV in coasting braking is provided by the hydraulic braking system. Fig. 14 shows the simulation results of the hydraulic coasting braking control of the EV and the reference vehicle. The acceleration curves are shown in Figs. 14(a) and 14(b) at the initial speed of 100 km/h and 50 km/h, respectively. It is obvious that the acceleration curves of the two vehicles are coincident with each other, which means that the two vehicles have the similar coasting driving feelings.

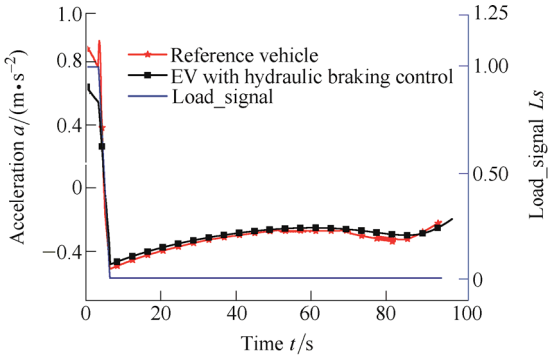

(a) Acceleration contrast at initial speed of 100 km/h

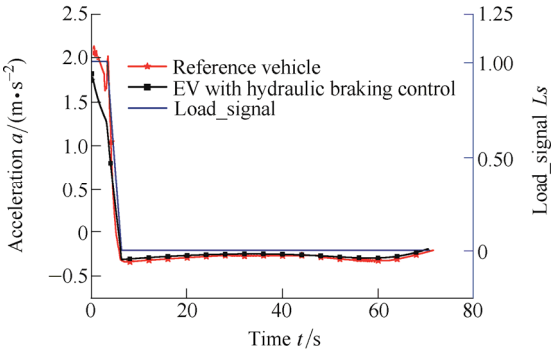

(b) Acceleration contrast at inital speed of 50 km/h

Fig. 14.　Hydraulic coasting braking control of the EV

7　Hardware-in-loop Experiment and Result Analysis

For the control unit, the real-time performance is very important. Due to the low cost, high accuracy and simplicity, the hardware-in-loop experiment is widely used to validate the real-time performance of the control unit[17–18].

Based on dSPACE, the hardware-in-loop experiment is conducted to testify the effectiveness of the coasting control algorithm. The whole vehicle model is compiled and downloaded to the DS1006 board and the control algorithm is compiled and downloaded to the Micro AutoBox to transform to the rapid control prototype (RCP)[19]. Controller area network (CAN) is used for the signal communication between Micro Autobox and DS1006[20]. The CAN communication protocol is ISO11898. The simulation step is set to 0.001 second. The ControlDesk displays vehicle status, such as speed, acceleration, battery SOC, and so on. The physical connection of the simulation test is shown as Fig. 15.

The comparisons of experiment results concerning speed and acceleration at the initial speed of 50 km/h and 100 km/h are shown as Fig. 16 and Fig. 17, respectively. It is evident that the speed and acceleration of EV have the same trend with that of the reference vehicle under different battery SOC, so the similar driving feeling can be ensured for the EV. Moreover, the real-time experiment results are coincident with that of the off-line simulation discussed above, so the real-time performance of the control algorithm is validated.

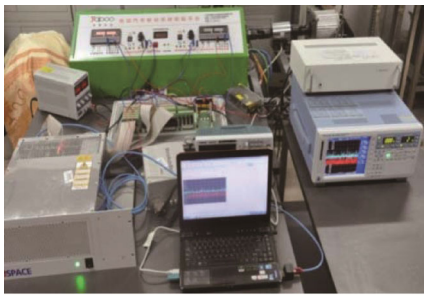

Fig. 15. Hardware-in-loop physical connection

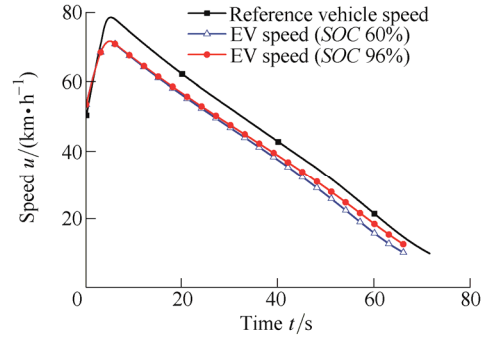

(a) Speed contrast

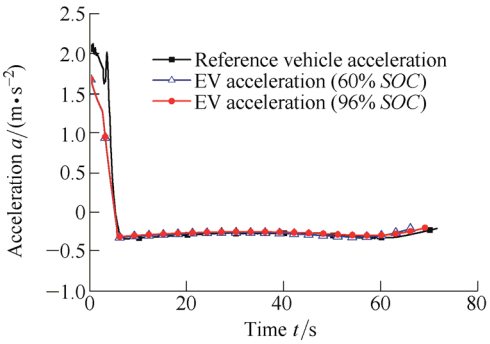

(b) Acceleration contrast

Fig. 16. Experiment result at initial speed of 50 km/h

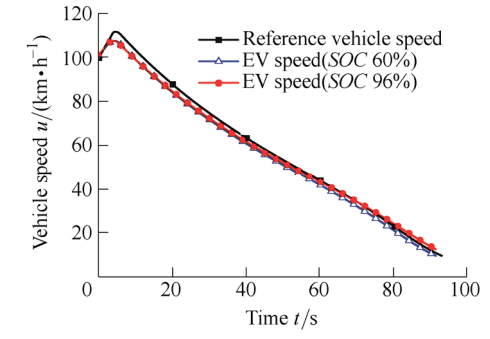

(a) Speed contrast

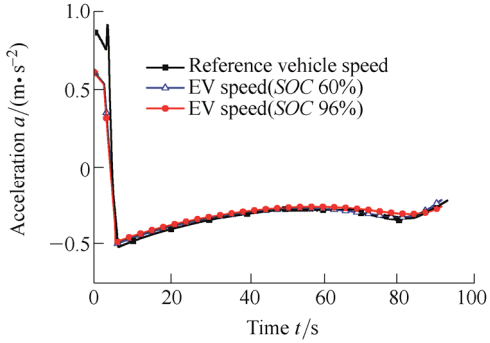

(b) Acceleration contrast

Fig. 17. Experiment result contrast at initial speed of 100 km/h

8 Conclusions

(1) By controlling the motor braking torque or hydraulic torque, the EV can achieve the similar driving feeling to that of the reference vehicle in coasting mode.

(2) When the battery SOC is below 95%, the EV can realize the coasting braking effect by using motor braking, and the battery SOC will increase by 0.036% and 0.021 2%, respectively at the initial speed of 100 km/h and 50 km/h.

(3) The control algorithm with the advantage of simplicity and practicality is proposed, and its real-time performance is validated through the hard-in-loop experiment.

References

[1] PÉREZ J, NASHASHIBI F, LEFAUDEUX B, et al. Autonomous docking based on infrared system for electric vehicle charging in urban areas[J]. *Sensors*, 2013, 13(2): 2645–2663.

[2] NOZAWA T, SHAMOTO S, KATANODA T. Development of electric vehicle system for city commuter vehicle[C]//*SAE 2013 World Congress and Exhibition*, Detroit, MI, USA, April 16-182013: No.2013-01-1447.

[3] GAO Y M, CHU L, EHSANI M. Design and control principles of hybrid braking system for EV, HEV and FCV[C]//*Vehicle Power and Propulsion Conference*, Arlington, Texas, USA, Sept. 9–12, 2007: 384–391.

[4] ZHAO X, YUAN X L, YU Q. Research of driving performance for heavy duty vehicle running on long downhill road based on engine brake[J]. *Open Mechanical Engineering Journal*, 2014, 8: 475–479.

[5] WANG M, SUN Z C, ZHUO G R, et al. Braking energy recovery system for electric vehicles[J]. *Nongye Jixie Xuebao(Transactions of the Chinese Society of Agricultural Machinery)*, 2012, 43(2): 6–10. (in Chinese)

[6] GU J, OUYANG M G, LI J Q, et al. Driving and braking control of PM synchronous motor based on low-resolution hall sensor for battery electric vehicle[J]. *Chinese Journal of Mechanical Engineering*, 2013, 26(1): 1–10.

[7] XU G Q, LI W M, XU K, et al. An intelligent regenerative braking strategy for electric vehicles[J]. *Energies*, 2011, 4(9): 1461–1477.

[8] BO L, CHENG Y Q. H∞ robust controller design for regenerative braking control of electric vehicles[C]//*Proceedings of the 2011 6th IEEE Conference on Industrial Electronics and Applications, ICIEA 2011*, Beijing, China, June 21–23, 2011: 214–219.

[9] YANG Y J, ZHAO H, ZHU M F. A study on the control strategy for maximum energy recovery by regenerative braking in electric vehicles[J]. *Automotive Engineering*, 2013, 35(2): 105–110. (in Chinese)

[10] HUANG W Y, CHENG Y, CAO H, et al. Development of EV's energy feedback control strategy referring to Jinan's vehicle driving-cycle[J]. *Electric Machines and Control*, 2012, 16(10): 86–94.

[11] WANG F, ZHUO B. Regenerative braking strategy for hybrid electric vehicles based on regenerative torque optimization control[J]. *Proceedings of the Institution of Mechanical Engineers, Part D: Journal of Automobile Engineering*, 2008, 222(4): 499–513.

[12] WANG F, ZHONG H, MA Z L, et al. Regenerative braking of hybrid power system in coasting mode[J]. *Huanan Ligong Daxue Xuebao/Journal of South China University of Technology (Natural Science)*, 2009, 37(7): 62–68. (in Chinese)

[13] SUN L. *Study on drier braking intention identification and control algorithm for HEV*[D]. Changchun: Jilin University, 2010. (in Chinese)

[14] CIKANEK S R, BAILEY K E. Regenerative braking system for a hybrid electric vehicles[C]//*Proceedings of the American Control Conference*, Anchorage, AK, USA, May 8–10, 2002: 3129–3134.
[15] LU D B. *Study on permanent magnet brushless hub motor drive system control for four-wheel drive electric vehicle*[D]. Beijing: Tsinghua University, 2012. (in Chinese)
[16] CHEN C A, LIN M C. Adaptive-learning regeneration controller design for electric vehicles[C]//*SAE 2013 World Congress and Exhibition*, Detroit, MI, USA, April 16–18, 2013: No. 2013-32-9018.
[17] LI H Z, LI L, SONG J, et al. Algorithm for calculating torque base in vehicle traction control system[J]. *Chinese Journal of Mechanical Engineering*, 2012, 25(6): 1130–1137.
[18] ZHANG W, DING N G, CHEN M R, et al. Development of a low-cost hardware-in-the-loop simulation system as a test bench for anti-lock braking system[J]. *Chinese Journal of Mechanical Engineering*, 2011: 98–104.
[19] OU J, KANG X P, ZHANG Y, et al. Design of rapid control prototype for vehicle stability[J]. *Computer Simulation*, 2009, 26(6): 318–321. (in Chinese)
[20] ZHANG C N, WU J B, ZOU Y, et al. Hardware-in-the-loop simulation on control strategy in hybrid electric transmission tracked vehicle[J]. *Transactions of Beijing Institute of Technology*, 2009, 29(9): 790–794. (in Chinese)

Biographical notes

SUN Daxu, born in 1973, is currently a PhD candidate at *School of Mechanical & Automotive Engineering, South China University of Technology, China*. He obtained his Master degree from *Henan Polytechnic University, China*, in 2006. His research interests include system modeling and simulation for EV and the application of modern control theory in EV control system.
E-mail: sundx55@126.com

LAN Fengchong, born in 1959, is a professor at *School of Mechanical & Automotive Engineering, South China University of Technology, China*. He obtained his PhD degree from *Jilin University, China*, in 1998. His research interests include automotive body structure and safety and automotive occupant's thermal comfort performance.
Tel: +86-20-87113955; E-mail: fclan@scut.edu.cn

ZHOU Yunjiao, born in 1982, is a lecturer at *School of Mechanical & Automotive Engineering, South China University of Technology, China*. He obtained his PhD degree from *South China University of Technology, China*, in 2011. His research interests include system modeling and simulation for EV, lightweight and crashworthiness design of car body structure.
Tel: +86-20-87113955; E-mail: mezhouyj@scut.edu.cn

CHEN Jiqing, born in 1966, is a professor at *School of Mechanical & Automotive Engineering, South China University of Technology, China*. She obtained her PhD degree from *Salford University, UK*, 2005 and *Jilin University, China*, in 1998. Her research interests include lightweight and crashworthiness design of car body structure, simulation and theory of occupant's thermal comfort.
Tel: +86-20-87113955; E-mail: chjq@scut.edu.cn